SCIENCE CHINA
Technological Sciences

May 2013 Vol.56 No.5: 1102–1111
doi: 10.1007/s11431-013-5188-3

Formation keeping control through inter-satellite electromagnetic force

CAI WeiWei*, YANG LePing, ZHU YanWei & ZHANG YuanWen

College of Aerospace Science and Engineering, National University of Defense Technology, Changsha 410073, China

Received October 10, 2012; accepted March 7, 2013; published online March 31, 2013

Satellite formation keeping through inter-satellite electromagnetic force provides an attractive alternative for future space missions due to its distinct advantages of no propellant consumption or plume contamination as compared to conventional approaches. However, the internal force nature as well as the high nonlinearity and coupling of electromagnetic force brings new control challenges for this novel technique. In this paper, analysis on the dynamics characteristics and special control issues in the presence of electromagnetic force is carried out on the basis of the derived relatively translational dynamics. Considering the model uncertainties, external disturbances and sensor noise, a combined nonlinear control scheme involving feed-forward and feedback control components is proposed for electromagnetic-force-based formation keeping. The feed-forward component is directly obtained through desired configuration and dynamics under nominal conditions while the feedback component is realized utilizing active disturbance rejection control methodology with some reasonable improvement. Numerical simulation is presented to verify the feasibility and validity of the combined control scheme.

inter-satellite electromagnetic force, formation keeping, dynamics analysis, active disturbance rejection, nonlinear control

Citation: Cai W W, Yang L P, Zhu Y W, et al. Formation keeping control through inter-satellite electromagnetic force. Sci China Tech Sci, 2013, 56: 1102–1111, doi: 10.1007/s11431-013-5188-3

1 Introduction

Satellite formation flying (SFF) has been identified as a promising technology for many future space missions due to its attractive prospect including cost reduction, redundancy, upgradeability and performance improvement. A desired formation configuration is necessary to fulfill the mission goal, yet practical implementation of SFF relies on accurate control of the relative position and orientation, which is still a main challenge. To date, many space missions utilizing SFF have been designed to control the formation via conventional propellant-based actuators. However, the inherent shortcomings of these actuators including propellant consumption, vibration caused by propellant tank and plume contamination would lead to degraded formation performance, such as limited lifetime, complicated attitude control, and unqualified imaging of optical payload. An emerging novel technique named Electromagnetic Formation Flying (EMFF) offers an attractive alternative. The key to EMFF lies on the utilization of electromagnetic force and torque generated by a set of orthogonal electric coils to control the relative separation and attitude. The inter-satellite electromagnetic force can not only effectively avoid the shortcomings of conventional thrusters, but also offer continuous, reversible and synchronous control, which ensures a promising prospect of accurate formation control. Nevertheless, EMFF is a structurally coupled system, which means the state evolution of one member is highly related to the state of others when the electromagnetic coils are activated. Together with the high nonlinearity of electromagnetic force,

*Corresponding author (email: tsaiweiwei@163.com)

challenges for the formation control of EMFF are greatly increased. In this work, we concentrate on the issues of formation keeping control through inter-satellite electromagnetic force.

As the leading research institute of EMFF, the Space Systems Laboratory at MIT has conducted a series of studies on the concept, system design, dynamics and control of EMFF. Kwon introduced the novel applications of EMFF in future missions, and studied the system design of EMFF [1]. Schweighart and Sedwick investigated the exact and approximate models for the electromagnetic force and torques, as well as the magnetic dipole solution planning approaches [2]. Elias derived the nonlinear dynamics model of EMFF through Kane's method and analyzed the stability and controllability of the linearized equations of motion [3]. Ahsun et al. presented the dynamics for EMFF in Near-Earth Orbits, and proposed a nonlinear adaptive controller [4, 5]. A proof-of-concept ground testbed consisting of two vehicles with high temperature superconducting wire and reaction wheels was built to demonstrate the controllability to achieve different maneuvers [6, 7]. Analogous idea was independently proposed and investigated by groups at the University of Tokyo. Kaneda et al. proposed to counteract the geomagnetic disturbance torques of EMFF with sinusoidal current of different phases [8]. Additionally, Polish researchers Wawrzaszek and Banaszkiewicz studied the application of EMFF to interferometric missions which include two or three aligned satellites rotating around the array's mass center [9]. Zeng and Hu analyzed the effects of the Earth's magnetic field on electromagnetic satellites, and proposed a robust sliding mode controller for electromagnetic formations of fractionated spacecraft [10]. Feng et al. designed a nonlinear control law for EMFF based on saturation function [11]. Su and Dong investigated the station-tracking problem of EMFF [12].

In the field of traditional SFF, various approaches for formation keeping and reconfiguration control have been studied in the past years, such as adaptive control [13], sliding mode control [14, 15], distributed control [16] and Null-Space Based behavioral control [17]. However, the control problem for satellite formations through inter-satellite force has not yet been systematically studied. Based on a brief analysis of the special dynamic property and control issues, we propose a combined control strategy comprising feed-forward and feedback components for formation keeping of EMFF, considering uncertainties, various disturbances and sensor noise. The feed-forward control component that keeps the desired formation configuration is simply derived by inverse dynamics, while the feedback control component compensates for any deviation of the configuration. The feedback control component is designed utilizing Active Disturbance Rejection Control (ADRC), which has great benefits in active rejection of both internal and external disturbances [18]. It is applicable to high order, nonlinear, time-varying, multi-input and multi-output systems, and has been successfully used in numerous applications [19, 20]. The fundamental idea of ADRC is to estimate the system dynamics and the total disturbances, which are extended as a new system state in real time with an Extended State Observer (ESO), and to compensate for them. Considering the sensitivity of ESO with respect to sensor noise, we designed a modified ESO integrating input filtration function. Taking the robust capability of sliding mode control, we also proposed an alternative nonlinear compensation control block for the original ADRC methodology to improve the system's robustness. Our main contribution includes an analysis of the dynamic characteristic and special issues of EMFF, and a combined control strategy for formation keeping based on active disturbance rejection. We make some improvement to the original ADRC methodology, and expand its application to the novel satellite formation with inter-satellite electromagnetic force. And effects of the sensor noise are considered in design of the controller.

The remainder of the paper is organized as follows. Firstly, the translational dynamic model for a formation with inter-satellite electromagnetic force is developed, and then an analysis on the dynamics property and formation keeping challenge is briefly conducted in Section 2. Secondly, the design of a combined formation keeping controller is investigated, and improvements to the original ADRC methodology are given in detail in Section 3. Thirdly, Section 4 gives numerical simulation on an example formation configuration to validate the feasibility of the control strategy. Some usefully conclusions are given in Section 5.

2 Dynamic modeling and analysis

In the following subsections, dynamic equations for the relatively translational motion of electromagnetic satellites are derived, and dynamics analysis and special control issues are presented in brief.

2.1 Coordinates and transformations

The electromagnetic force does not change the total inertial formation angular momentum vector due to its internal force nature. Thus it is convenient to describe the relative motion of electromagnetic satellites in the rotating Hill orbit frame $\boldsymbol{H}$-xyz whose origin is chosen to be at the center of mass of the formation as shown in Figure 1. The Cartesian x, y and z coordinates are aligned with the directions of the orbit radial (outward), orbital velocity vector and normal vector with respect to the orbital plane. To calculate the electromagnetic force, a formation fixed coordinate frame $\boldsymbol{B}$-$x'y'z'$ is defined with its origin also located at the center of mass of the formation. The $x'y'$ plane coincides with the formation plane, the x' axis is aligned with the line of sight (LOS) vector from *Sat*A to *Sat*B and the y' axis is vertical to

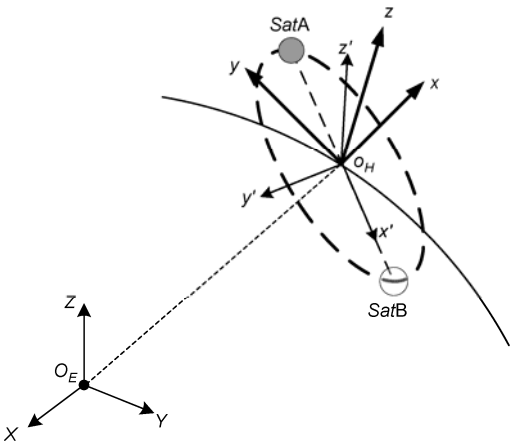

Figure 1 Geometry of the Cartesian coordinate frames.

x' axis. The z' axis is normal to the formation plane so as to complete the right-hand triad.

It is necessary to introduce the transformation between frames $\boldsymbol{B}$ and $\boldsymbol{H}$ since the electromagnetic force and translational dynamics are derived in these two different frames respectively. Taking the xy plane as the reference formation plane, any other formation plane can be obtained by rotating frame $\boldsymbol{H}$ about the x axis through Euler angle θ_x and the new y axis through θ_y in sequence. Since the $x'y'$ plane coincides with the formation plane, the orientation of frame $\boldsymbol{B}$ with respect to frame $\boldsymbol{H}$ can be expressed by Euler angles (θ_x, θ_y, γ) as shown in Figure 2, where γ represents the phase angle of the LOS vector.

Define the matrix $\boldsymbol{L}$ as

$$\boldsymbol{L}=\boldsymbol{R}_2\left(\theta_y\right)\boldsymbol{R}_1\left(\theta_x\right)=\left[L_{ij}\right],\quad \left(i,j=1,\ 2,\ 3\right), \tag{1}$$

where $\boldsymbol{R}_1$ and $\boldsymbol{R}_2$ indicate the unit Euler rotation matrix, and $\boldsymbol{L}$ would be a constant matrix if the formation plane remains unchanged.

The resultant transformation matrix $\boldsymbol{M}$ from the Hill orbital frame $\boldsymbol{H}$ to the formation fixed frame $\boldsymbol{B}$ is given as

$$\boldsymbol{M}=\boldsymbol{R}_3\left(\gamma\right)\boldsymbol{R}_2\left(\theta_y\right)\boldsymbol{R}_1\left(\theta_x\right)=\left[M_{ij}\right],\ \left(i,j=1,\ 2,\ 3\right). \tag{2}$$

Note that the matrix $\boldsymbol{M}$ is a time-varying matrix.

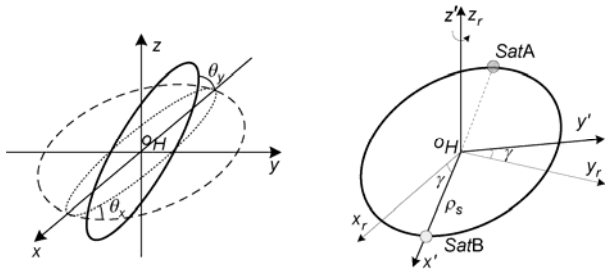

Figure 2 Illustration of the coordinate transformation.

2.2 Electromagnetic force model

The exact model of electromagnetic force contains a series of complicated integrations in the formula, making it inappropriate for formation controller design. When the electromagnetic satellites separate by at least 6–8 times the coil radii, the far-field model obtained by employing first order Taylor expansion formula is an alternative for controller design [2]. According to the dipole approximations for electromagnet interactions, the electromagnetic mechanism on each satellite is modeled as one large magnetic dipole with the orthogonal vector components illustrated as in Figure 3.

The electromagnetic force acting on *Sat*A due to *Sat*B is given by [4]

$$\boldsymbol{F}_{\mathrm{EA}}=\frac{3\mu_0}{4\pi}\left[-\frac{\boldsymbol{\mu}_{\mathrm{A}}\boldsymbol{\mu}_{\mathrm{B}}}{r^5}\boldsymbol{r}-\frac{\boldsymbol{\mu}_{\mathrm{A}}\boldsymbol{r}}{r^5}\boldsymbol{\mu}_{\mathrm{B}}-\frac{\boldsymbol{\mu}_{\mathrm{B}}\boldsymbol{r}}{r^5}\boldsymbol{\mu}_{\mathrm{A}}+5\frac{\left(\boldsymbol{\mu}_{\mathrm{A}}\boldsymbol{r}\right)\left(\boldsymbol{\mu}_{\mathrm{B}}\boldsymbol{r}\right)}{r^7}\boldsymbol{r}\right], \tag{3}$$

where $\boldsymbol{\mu}_{\mathrm{A}}$ and $\boldsymbol{\mu}_{\mathrm{B}}$ represent the magnetic dipole vectors on *Sat*A and *Sat*B respectively, $\boldsymbol{r}$ is the relative position vector along LOS, and the permeability of free space is $\mu_0=4\pi\times 10^{-7}$ Tm A^{-1}.

For a given electromagnetic force, there may exist various dipole solutions of $\boldsymbol{\mu}_{\mathrm{A}}$ and $\boldsymbol{\mu}_{\mathrm{B}}$, resulting in enhancive difficulty in designing controller [2]. Thus for the sake of simplicity, it is assumed that the magnetic dipole on *Sat*A aligns with the LOS vector all through the mission process. The magnetic dipoles $\boldsymbol{\mu}_{\mathrm{A}}$, $\boldsymbol{\mu}_{\mathrm{B}}$ and relative position vector $\boldsymbol{r}$ in the frame $\boldsymbol{B}$ can be expressed as

$$\boldsymbol{\mu}_{\mathrm{A}}=\left[\mu_{\mathrm{A}},0,0\right]^{\mathrm{T}},\boldsymbol{\mu}_{\mathrm{B}}=\left[\mu_{\mathrm{Bx'}},\mu_{\mathrm{By'}},\mu_{\mathrm{Bz'}}\right]^{\mathrm{T}},\ \boldsymbol{r}=\left[d,0,0\right]^{\mathrm{T}}. \tag{4}$$

Projections of the electromagnetic force acting on *Sat*A in frame $\boldsymbol{B}$ can be easily derived by substituting eq. (4) into eq. (3)

$$\begin{aligned}\boldsymbol{F}_{\mathrm{EA}}&=\left[F_{\mathrm{EAx'}}\quad F_{\mathrm{EAy'}}\quad F_{\mathrm{EAz'}}\right]^{\mathrm{T}}\\&=\frac{3\mu_0\mu_{\mathrm{A}}}{4\pi d^4}\left[2\mu_{\mathrm{Bx'}}\quad -\mu_{\mathrm{By'}}\quad -\mu_{\mathrm{Bz'}}\right]^{\mathrm{T}}.\end{aligned} \tag{5}$$

2.3 Relatively translational dynamics

Satellite clusters usually contain several satellites, and the electromagnetic force acting on each member is generated

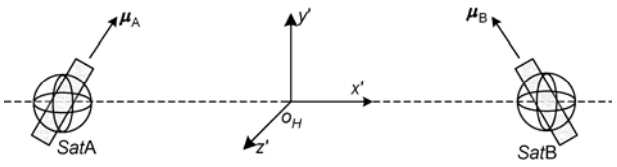

Figure 3 Three-dimensional model of magnetic dipole.

by all the others in the formation. In our research, only the relative motion of two electromagnetic satellites is considered since it could be viewed as a sub-problem of a multi-satellite formation flight problem. The center of mass of the formation can be reasonably assumed to move in a near-circular reference orbit since it is uncontrollable in the presence of electromagnetic force. Moreover, the effects of the oblateness of the Earth are neglected in this section.

The inertial motions of both satellites in the inertial frame are given as

$$\begin{cases} m_{\mathrm{A}}\ddot{\boldsymbol{R}}_{\mathrm{A}}+\dfrac{\mu_e m_{\mathrm{A}}\boldsymbol{R}_{\mathrm{A}}}{R_{\mathrm{A}}^3}=\boldsymbol{F}_{\mathrm{A}}^{\mathrm{m}}+\boldsymbol{F}_{\mathrm{dA}}, \\ m_{\mathrm{B}}\ddot{\boldsymbol{R}}_{\mathrm{B}}+\dfrac{\mu_e m_{\mathrm{B}}\boldsymbol{R}_{\mathrm{B}}}{R_{\mathrm{B}}^3}=\boldsymbol{F}_{\mathrm{B}}^{\mathrm{m}}+\boldsymbol{F}_{\mathrm{dB}}, \end{cases} \tag{6}$$

where $\boldsymbol{F}^{\mathrm{m}}$ is the inter-satellite electromagnetic force, and $\boldsymbol{F}_{\mathrm{d}}$ is the external disturbance force in space.

The second-order derivation of relative separation vector $\boldsymbol{r}$ can be written as

$$\begin{aligned} \ddot{\boldsymbol{r}} &= \ddot{\boldsymbol{R}}_{\mathrm{A}}-\ddot{\boldsymbol{R}}_{\mathrm{B}} \\ &= -\frac{\mu_e}{R_{\mathrm{A}}^3}\boldsymbol{R}_{\mathrm{A}}+\frac{\mu_e}{R_{\mathrm{B}}^3}\boldsymbol{R}_{\mathrm{B}}+\frac{\boldsymbol{F}_{\mathrm{A}}^{\mathrm{m}}}{m_{\mathrm{A}}}-\frac{\boldsymbol{F}_{\mathrm{B}}^{\mathrm{m}}}{m_{\mathrm{B}}}+\frac{\boldsymbol{F}_{\mathrm{dA}}}{m_{\mathrm{A}}}-\frac{\boldsymbol{F}_{\mathrm{dB}}}{m_{\mathrm{B}}}. \end{aligned} \tag{7}$$

According to the derivation of Hill equations, the relative motion of *Sat*A to *Sat*B in frame $\boldsymbol{H}$ can be obtained as

$$\begin{cases} \ddot{x}-2\omega_0\dot{y}-3\omega_0^2 x=\dfrac{1}{m_{\mathrm{A}}}F_{\mathrm{A}x}^{\mathrm{m}}-\dfrac{1}{m_{\mathrm{B}}}F_{\mathrm{B}x}^{\mathrm{m}}+\Delta f_{\mathrm{d}x}, \\ \ddot{y}+2\omega_0\dot{x}=\dfrac{1}{m_{\mathrm{A}}}F_{\mathrm{A}y}^{\mathrm{m}}-\dfrac{1}{m_{\mathrm{B}}}F_{\mathrm{B}y}^{\mathrm{m}}+\Delta f_{\mathrm{d}y}, \\ \ddot{z}+\omega_0^2 z=\dfrac{1}{m_{\mathrm{A}}}F_{\mathrm{A}z}^{\mathrm{m}}-\dfrac{1}{m_{\mathrm{B}}}F_{\mathrm{B}z}^{\mathrm{m}}+\Delta f_{\mathrm{d}z}, \end{cases} \tag{8}$$

where x, y, z are components of the relatively positive vector in frame $\boldsymbol{H}$, ω_0 is the orbital angular velocity of the formation mass center, and Δf_{d} represents the difference of disturbance acceleration.

Since the electromagnetic force is in nature an internal force, it is bound by Newton's third law,

$$\boldsymbol{F}_{\mathrm{B}}^{\mathrm{m}}=-\boldsymbol{F}_{\mathrm{A}}^{\mathrm{m}}. \tag{9}$$

The relatively translational dynamics can be rearranged by substituting eq. (9) into eq. (8) as

$$\begin{cases} \ddot{x}-2\omega_0\dot{y}-3\omega_0^2 x=F_{\mathrm{A}x}^{\mathrm{m}}/\bar{M}+\Delta f_{\mathrm{d}x}, \\ \ddot{y}+2\omega_0\dot{x}=F_{\mathrm{A}y}^{\mathrm{m}}/\bar{M}+\Delta f_{\mathrm{d}y}, \\ \ddot{z}+\omega_0^2 z=F_{\mathrm{A}z}^{\mathrm{m}}/\bar{M}+\Delta f_{\mathrm{d}z}, \end{cases} \tag{10}$$

where $\bar{M}=m_{\mathrm{A}}m_{\mathrm{B}}/(m_{\mathrm{A}}+m_{\mathrm{B}})$ denotes the equivalent mass of the electromagnetic formation system.

2.4 Dynamic analysis and control issues

A brief analysis of the derived dynamic model is summarized here to reveal the unique dynamic properties and control challenges of EMFF.

1) The coupling in the dynamic model can be approached from two perspectives. The first one is due to the internal nature of electromagnetic force. Since the electromagnetic force acts on both satellites synchronously, changing the magnitude or orientation of one magnetic dipole would affect the motion of both satellites. The second one is induced by the electromagnetic force and the relative separation. It is evident in eqs. (3) and (8) that the magnitude of the electromagnetic force is partly dependent on relative separation, whereas the force provides the changing acceleration of relative separation.

2) Generally, the magnitude and orientation of the electromagnetic force depend upon the product of magnetic dipole on both satellites; and the magnitude goes down with distance to the fourth power. These nonlinearities may bring difficulties to the controller design.

3) Due to the complexity of exact electromagnetic force model, only the far-field model is used to deduce the dynamic model. The far-field model is essentially an approximation of the exact model, leading to model uncertainties of the translational dynamics. Moreover, the influence of the geomagnetic field brings additional environmental uncertainty. These uncertainties should be explicitly taken into account in the formation keeping control scheme.

3 Formation keeping control scheme

All the satellites in an EMFF are subject to external disturbances like atmospheric drag, solar radiation pressure, Earth's oblateness and geomagnetic field influence, resulting in inevitable damages on the formation configuration [19]. The formation keeping control objective is to design a controller that enables the formation to maintain a desired configuration in the presence of external disturbances, model uncertainties and sensor noise. However, the challenge is highlighted due to the inherent coupled characteristics of the dynamic model and the nonlinearity of electromagnetic force as discussed above. In this section, a combined control strategy is proposed comprising two terms

$$\boldsymbol{u}=\boldsymbol{u}_s+\boldsymbol{u}_e. \tag{11}$$

Here the first term is the feed-forward control component that maintains the desired formation configuration under nominal conditions, while the second is the feedback component that eliminates the configuration deviation. Architecture for the combined control strategy is illustrated in Figure 4.

3.1 Feed-forward control component

For the sake of convenience, a circular formation configura-

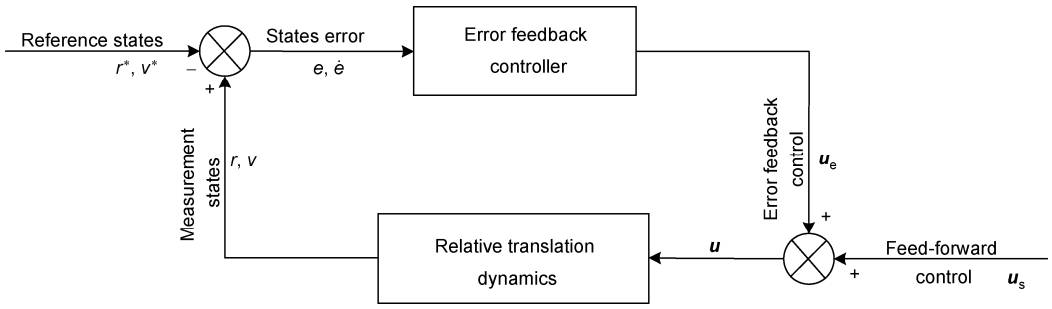

Figure 4 Architecture for the combined control strategy.

tion is taken as an example here, thus the relative position vector in the frame $\boldsymbol{B}$ from *Sat*B to *Sat*A can be written as

$$\boldsymbol{r}_{\mathrm{AB}}^{\boldsymbol{B}}=\left[-2\rho_s \quad 0 \quad 0\right]^{\mathrm{T}}. \tag{12}$$

Note that the superscript $\boldsymbol{B}$ indicates that the vector is expressed in frame $\boldsymbol{B}$.

According to the coordinate transformation relationship in eq. (2), the expression for the relative position vector in frame $\boldsymbol{H}$ can be written as

$$\boldsymbol{r}_{\mathrm{AB}}^{\boldsymbol{H}}=\begin{bmatrix}x\\y\\z\end{bmatrix}=\begin{bmatrix}-2\rho_s L_{11}\cos\gamma-2\rho_s L_{12}\sin\gamma\\-2\rho_s L_{21}\cos\gamma-2\rho_s L_{22}\sin\gamma\\2\rho_s L_{31}\cos\gamma+2\rho_s L_{32}\sin\gamma\end{bmatrix}. \tag{13}$$

Likewise, the superscript $\boldsymbol{H}$ denotes a vector expressed in frame $\boldsymbol{H}$.

Differentiating the relative states with respect to time yields

$$\begin{cases}\dot{x}=2\omega\rho_s L_{11}\sin\gamma-2\omega\rho_s L_{12}\cos\gamma,\\ \dot{y}=2\omega\rho_s L_{21}\sin\gamma-2\omega\rho_s L_{22}\cos\gamma,\\ \dot{z}=-2\omega\rho_s L_{31}\sin\gamma+2\omega\rho_s L_{32}\cos\gamma,\end{cases}\qquad \begin{cases}\ddot{x}=-\omega^2 x,\\ \ddot{y}=-\omega^2 y,\\ \ddot{z}=-\omega^2 z,\end{cases} \tag{14}$$

where ω represents the spinning angular velocity of the desired circular formation.

Since the control objective of the feed-forward control component is to maintain the desired configuration under nominal conditions, terms of disturbance acceleration in eq. (10) are neglected here:

$$\begin{cases}\ddot{x}-2\omega_0\dot{y}-3\omega_0^2 x=F_{\mathrm{A}sx}^{\mathrm{m}}/\bar{M},\\ \ddot{y}+2\omega_0\dot{x}=F_{\mathrm{A}sy}^{\mathrm{m}}/\bar{M},\\ \ddot{z}+\omega_0^2 z=F_{\mathrm{A}sz}^{\mathrm{m}}/\bar{M}.\end{cases} \tag{15}$$

Substituting eqs. (13) and (14) into eq. (15) yields the feed-forward electromagnetic force in frame $\boldsymbol{H}$ as

$$\begin{cases}F_{\mathrm{A}sx}^{\mathrm{m}H}=2\bar{M}\rho_s\left[\cos\gamma\left(\omega^2 L_{11}+3\omega\omega_0 L_{22}+3\omega_0^2 L_{11}\right)\right.\\ \qquad\left.+\sin\gamma\left(\omega^2 L_{12}-3\omega\omega_0 L_{21}+3\omega_0^2 L_{12}\right)\right],\\ F_{\mathrm{A}sy}^{\mathrm{m}H}=2\bar{M}\rho_s\left[\cos\gamma\left(\omega^2 L_{21}-2\omega\omega_0 L_{12}\right)\right.\\ \qquad\left.+\sin\gamma\left(\omega^2 L_{22}+2\omega\omega_0 L_{11}\right)\right],\\ F_{\mathrm{A}sz}^{\mathrm{m}H}=2\bar{M}\rho_s\left[\cos\gamma\left(\omega^2 L_{31}-\omega_0^2 L_{31}\right)\right.\\ \qquad\left.+\sin\gamma\left(\omega^2 L_{32}-\omega_0^2 L_{32}\right)\right].\end{cases} \tag{16}$$

Since the electromagnetic force is easy to compute in frame $\boldsymbol{B}$, the feed-forward electromagnetic control force above is transformed as

$$\begin{bmatrix}F_{\mathrm{A}sx'}^{\mathrm{m}B}\\F_{\mathrm{A}sy'}^{\mathrm{m}B}\\F_{\mathrm{A}sz'}^{\mathrm{m}B}\end{bmatrix}=\begin{bmatrix}M_{11}F_{\mathrm{A}sx}^{\mathrm{m}H}+M_{12}F_{\mathrm{A}sy}^{\mathrm{m}H}+M_{13}F_{\mathrm{A}sz}^{\mathrm{m}H}\\M_{21}F_{\mathrm{A}sx}^{\mathrm{m}H}+M_{22}F_{\mathrm{A}sy}^{\mathrm{m}H}+M_{23}F_{\mathrm{A}sz}^{\mathrm{m}H}\\M_{31}F_{\mathrm{A}sx}^{\mathrm{m}H}+M_{32}F_{\mathrm{A}sy}^{\mathrm{m}H}+M_{33}F_{\mathrm{A}sz}^{\mathrm{m}H}\end{bmatrix}. \tag{17}$$

Substituting eq. (17) into eq. (5) yields the feed-forward control component in the format of magnetic dipole on *Sat*B

$$\boldsymbol{u}_s=\begin{bmatrix}\mu_{\mathrm{B}sx'}\\\mu_{\mathrm{B}sy'}\\\mu_{\mathrm{B}sz'}\end{bmatrix}=\frac{64\pi\rho_s^4}{3\mu_0\mu_{\mathrm{A}}}\boldsymbol{DM}\begin{bmatrix}F_{\mathrm{A}sx}^{\mathrm{m}H}\\F_{\mathrm{A}sy}^{\mathrm{m}H}\\F_{\mathrm{A}sz}^{\mathrm{m}H}\end{bmatrix}, \tag{18}$$

where $\boldsymbol{D}$=diag([0.5, −1, −1]) is a constant diagonal matrix.

3.2 Feedback control component

The feedback control component for estimating the configuration deviation is proposed utilizing ADRC methodology. The essence of ADRC is to extend the internal and external disturbances as a new system state, and estimate them in a direct and real-time way through an ESO before compensation via disturbance rejection and nonlinear feedback. The architecture for feedback control component is as illustrated in Figure 5, and detailed design of each part and some reasonable improvements are described below.

(I) Equations of formation configuration deviation

The formation configuration deviation can be defined with the relative states error as

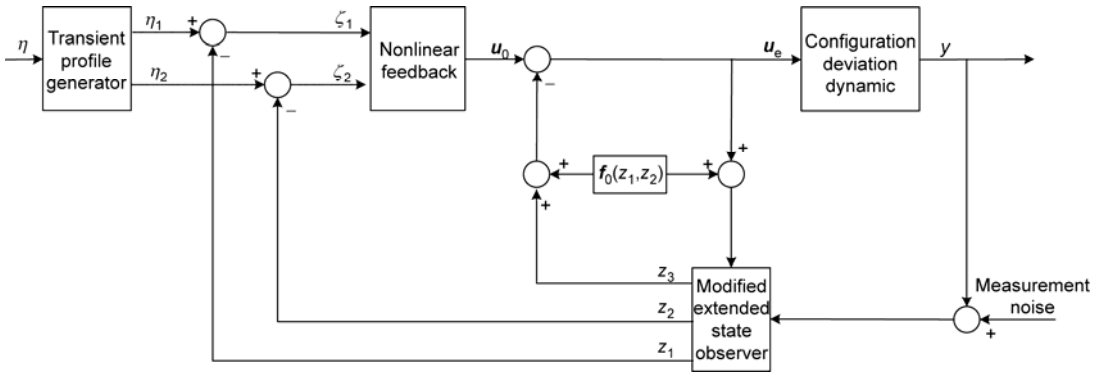

Figure 5 Diagram of feedback control component.

$$\begin{cases} \boldsymbol{e}(t)=\boldsymbol{\rho}(t)-\boldsymbol{\rho}^*(t), \\ \dot{\boldsymbol{e}}(t)=\dot{\boldsymbol{\rho}}(t)-\dot{\boldsymbol{\rho}}^*(t), \end{cases} \tag{19}$$

where $\boldsymbol{\rho}(t)=[x, y, z]^{\mathrm{T}}$ represents instant relative state vector satisfying eq. (10), and $\boldsymbol{\rho}^*(t)=[x^*, y^*, z^*]^{\mathrm{T}}$ is the desired state corresponding to feed-forward control under nominal conditions. Thus the equations of configuration deviation can be easily obtained as

$$\begin{cases} \ddot{e}_x-2\omega_0\dot{e}_y-3\omega_0^2e_x=f_{\mathrm{A}ex}^{\mathrm{m}}+\Delta f_{\mathrm{d}x}, \\ \ddot{e}_y+2\omega_0\dot{e}_x=f_{\mathrm{A}ey}^{\mathrm{m}}+\Delta f_{\mathrm{d}y}, \\ \ddot{e}_z+\omega_0^2e_z=f_{\mathrm{A}ez}^{\mathrm{m}}+\Delta f_{\mathrm{d}z}, \end{cases} \tag{20}$$

where $\boldsymbol{f}_{\mathrm{A}e}^{\mathrm{m}}=\boldsymbol{F}_{\mathrm{A}e}^{\mathrm{m}}/\bar{M}$ is the feedback control acceleration investigated in this section.

The dynamic equations above can be rearranged in the vector format as

$$\ddot{\boldsymbol{e}}=\boldsymbol{A}_1\boldsymbol{e}+\boldsymbol{A}_2\dot{\boldsymbol{e}}+\boldsymbol{f}_{\mathrm{A}e}^{\mathrm{m}}+\Delta\boldsymbol{f}_{\mathrm{d}}, \tag{21}$$

where $\boldsymbol{e}=\left[e_x,e_y,e_z\right]^{\mathrm{T}}$, $\boldsymbol{A}_1=\mathrm{diag}\left(\left[3\omega_0^2,0,-\omega_0^2\right]\right)$ and

$$\boldsymbol{A}_2=\begin{bmatrix} 0 & 2\omega_0 & 0 \\ -2\omega_0 & 0 & 0 \\ 0 & 0 & 0 \end{bmatrix}.$$

Define the states $\boldsymbol{x}_1$ and $\boldsymbol{x}_2$ as

$$\boldsymbol{x}_1=\boldsymbol{e}=\left[e_x,e_y,e_z\right]^{\mathrm{T}},$$
$$\boldsymbol{x}_2=\dot{\boldsymbol{e}}=\left[\dot{e}_x,\dot{e}_y,\dot{e}_z\right]^{\mathrm{T}}.$$

Eq. (21) can be given as

$$\begin{cases} \dot{\boldsymbol{x}}_1=\boldsymbol{x}_2, \\ \dot{\boldsymbol{x}}_2=\boldsymbol{f}\left(\boldsymbol{x}_1,\boldsymbol{x}_2\right)+\boldsymbol{v}_e+\boldsymbol{f}_{\mathrm{d}}, \\ \boldsymbol{y}=\boldsymbol{x}_1, \end{cases} \tag{22}$$

where $\boldsymbol{f}(\boldsymbol{x}_1, \boldsymbol{x}_2)=\boldsymbol{A}_1\boldsymbol{x}_1+\boldsymbol{A}_2\boldsymbol{x}_2$, $\boldsymbol{v}_e$ is the feedback control acceleration to be decided and $\boldsymbol{f}_{\mathrm{d}}$ denotes the external disturbance.

(II) Modified ESO and active disturbance rejection

Our objective here is to make the output $\boldsymbol{y}$ behavior as desired using $\boldsymbol{v}_e$ as the control input. However, the uncertainties of electromagnetic force model and environmental influence should be explicitly considered in the controller design. Taking the uncertainties of control input as additional disturbances acting on the system, we introduce a concept of total disturbance to denote the summation of all disturbances. Till now, our work is to design an ESO to eliminate the total disturbance for later active rejection. By extending the total disturbance as a new system state, the ESO estimates the dynamic states utilizing the system output $\boldsymbol{y}$ and control signal $\boldsymbol{v}_e$ as inputs. Nonetheless, the output $\boldsymbol{y}$, namely the relative navigation information, is inevitably affected by sensor noise. Thus we propose a modified ESO integrating a filtering function here.

Taking the sensor noise $\boldsymbol{n}_y$ and total disturbance $\boldsymbol{W}$ into account, the system model is given as

$$\begin{cases} \dot{\boldsymbol{x}}_1=\boldsymbol{x}_2, \\ \dot{\boldsymbol{x}}_2=\boldsymbol{f}\left(\boldsymbol{x}_1,\boldsymbol{x}_2\right)+\boldsymbol{v}_e+\boldsymbol{W}, \\ \boldsymbol{y}=\boldsymbol{x}_1+\boldsymbol{n}_y. \end{cases} \tag{23}$$

The output information is disposed by a one-order low-pass filter as

$$y_0=\frac{1}{\tau s+1}y, \tag{24}$$

where y_0 is the output signal of the filter, and τ is the design parameter of the filter.

Treating $\boldsymbol{W}$ as a new system state $\boldsymbol{x}_3$, and y_0 as a new state $\boldsymbol{x}_0$, the system model is now extended as

$$\begin{cases} \dot{\boldsymbol{x}}_0=\left(\boldsymbol{x}_1-\boldsymbol{x}_0\right)/\tau, \\ \dot{\boldsymbol{x}}_1=\boldsymbol{x}_2, \\ \dot{\boldsymbol{x}}_2=\boldsymbol{f}\left(\boldsymbol{x}_1,\boldsymbol{x}_2\right)+\boldsymbol{x}_3+\boldsymbol{v}_e, \\ \dot{\boldsymbol{x}}_3=\boldsymbol{\omega}_0(t), \\ \boldsymbol{y}=\boldsymbol{x}_0, \end{cases} \tag{25}$$

where $\boldsymbol{\omega}_0$ denotes $\dot{\boldsymbol{W}}$, which is unknown but bounded.

The ESO for the extended system above is [21]

$$\begin{cases} e_0 = z_0 - y, \\ \dot{z}_0 = (z_1 - z_0)/\tau - \beta_{00} e_0, \\ \dot{z}_1 = z_2 - \beta_{01} fal(e_0, \alpha_1, \delta_1), \\ \dot{z}_2 = z_3 - \beta_{02} fal(e_0, \alpha_2, \delta_2) + f_0(z_1, z_2) + v_e, \\ \dot{z}_3 = -\beta_{03} fal(e_0, \alpha_3, \delta_3), \end{cases} \tag{26}$$

where β_{0i} (i=0,⋯,3) are observer gains, and *fal* is the nonlinear function which is defined as [21]

$$fal(e, \alpha, \delta) = \begin{cases} e/\delta^{1-\alpha}, |e| \leqslant \delta, \\ |e|^{\alpha} \operatorname{sign}(e), |e| > \delta. \end{cases} \tag{27}$$

With proper observer gains and α_i, δ_i (i=0, ⋯, 3), outputs of the modified ESO z_i (i=0, ⋯, 3) would well track $\boldsymbol{y}_0$, $\boldsymbol{x}_1$, $\boldsymbol{x}_2$ and $\boldsymbol{W}$ respectively, making active rejection of the total disturbance possible.

Substituting the new control input

$$\boldsymbol{v}_0 = \boldsymbol{v}_e - \boldsymbol{f}(z_1, z_2) - z_3 \tag{28}$$

into the configuration deviation dynamics yields a reduced plant in the cascade integral form of

$$\begin{cases} \dot{\boldsymbol{x}}_1 = \boldsymbol{x}_2, \\ \dot{\boldsymbol{x}}_2 = \boldsymbol{v}_0, \\ \boldsymbol{y} = \boldsymbol{x}_1. \end{cases} \tag{29}$$

The disturbances are eliminated in eq. (29), and the control problem is transformed to choose a proper $\boldsymbol{v}_0$ for the new plant.

(III) Transient profile and nonlinear feedback

The purpose of introducing the transient profile is to guarantee the dynamic states or system outputs convergence to their desired value quickly and without overshoot. Different transient profiles have been devised by researchers for practical systems. Among them, Han proposed a simple tracking differentiator based approach which is easy-to-use with good performance [21]. In this paper, we have also generated the transient profile for formation configuration deviation utilizing the differentiator.

When it comes to the nonlinear feedback block, the original ADRC imposes the nonlinear functions *fal* and *fhan* to produce good results [21]. Nonetheless, it is not easy to select proper tuning parameters of these nonlinear functions for a multi-input and multi-output system. As an alternative, we propose a sliding mode controller here to compensate for the total disturbance estimated above.

Denoting the outputs of transient profile generator as $\boldsymbol{\eta}_1, \boldsymbol{\eta}_2 = \dot{\boldsymbol{\eta}}_1$, which are the desired transient profile of states $\boldsymbol{x}_1$ and $\boldsymbol{x}_2$, the tracking error of the real states to the transition profile can be defined as

$$\begin{cases} \boldsymbol{\zeta}_1 = \boldsymbol{\eta}_1 - \boldsymbol{z}_1, \\ \boldsymbol{\zeta}_2 = \boldsymbol{\eta}_2 - \boldsymbol{z}_2. \end{cases} \tag{30}$$

Together with eq. (29), the time derivative of the tracking error is given by

$$\begin{cases} \dot{\boldsymbol{\zeta}}_1 = \boldsymbol{\zeta}_2, \\ \dot{\boldsymbol{\zeta}}_2 = \boldsymbol{\eta}_3 - \boldsymbol{v}_0, \end{cases} \tag{31}$$

where $\boldsymbol{\eta}_3$ represents the desired second order transient profile.

The states of the control plant would track the transient profile well if the tracking error converges to zero, which is our objective here.

The sliding mode surface $\boldsymbol{s}$ is designed as [19]

$$\boldsymbol{s} = \boldsymbol{\zeta}_2 + \lambda \boldsymbol{\zeta}_1, \tag{32}$$

where λ is a positive constant parameter.

Set the reaching condition of the sliding surface as

$$\dot{\boldsymbol{s}} = -\boldsymbol{\varepsilon} sat(\boldsymbol{s}) - \boldsymbol{k}\boldsymbol{s}, \tag{33}$$

where $\boldsymbol{\varepsilon}$, $\boldsymbol{k}$ are the tuning parameters, and *sat* is the saturation function which is given as

$$sat(s) = \begin{cases} s/d, |s| \leqslant d, \\ sign(s), |s| \leqslant d, \end{cases} \tag{34}$$

where d is the thickness of the boundary layer, and $sign(s) = s/|s|$. The saturation function *sat* is imported to avoid the high-frequency chattering caused by the discontinuous nonlinearity function *sign*.

Taking eq. (31) into the time derivative of eq. (32) yields

$$\dot{\boldsymbol{s}} = \dot{\boldsymbol{\zeta}}_2 + \lambda \dot{\boldsymbol{\zeta}}_1 = \boldsymbol{\eta}_3 - \boldsymbol{v}_0 + \lambda \boldsymbol{\zeta}_2. \tag{35}$$

Substituting eq. (33) to eq. (35) yields the nonlinear states error feedback control law as

$$\boldsymbol{v}_0 = \boldsymbol{\eta}_3 + \lambda \boldsymbol{\zeta}_2 + \boldsymbol{\varepsilon} sat(\boldsymbol{s}) + \boldsymbol{k}\boldsymbol{s}. \tag{36}$$

Thus the feedback control input $\boldsymbol{v}_e$ could be written as

$$\boldsymbol{v}_e = \boldsymbol{\eta}_3 + \lambda \boldsymbol{\zeta}_2 + \boldsymbol{\varepsilon} sat(\boldsymbol{s}) + \boldsymbol{k}\boldsymbol{s} - z_3 - f(z_1, z_2). \tag{37}$$

According to the definition of error feedback control acceleration in eq. (20), the corresponding electromagnetic force can be obtained by the multiplication of the equivalent mass $\bar{M}$. Likewise, substituting the error feedback electromagnetic forces into eq. (5) yields the control input in the format of magnetic dipole.

4 Numerical simulation

Included in this section are numerical simulations for a two-

satellite electromagnetic formation keeping to evaluate the performance of the proposed combined control strategy. This example is motivated by the application of SFF in the synthetic aperture radar (SAR) mission, in which orbits of individual satellites are non-Keplerian requiring continuous formation keeping control to maintain the desired configuration [22]. The formation center of mass is assumed to be moving in a circular orbit at an altitude of 500 km; and the two identical satellites are designed to spin around the formation center of mass with a period of 2 h and the radius of 15 m. The mass of the satellite is 50 kg, and the magnetic dipole on *Sat*A aligning with LOS vector all the time is selected as a constant of 3×10^6 H m^{-1}. The initial values of Euler angles (θ_x, θ_y, γ) representing the transformation between frames $\boldsymbol{B}$ and $\boldsymbol{H}$ are ($\pi/6$, $\pi/6$, $\pi/18$), respectively. According to the assumption of unvaried orientation of the formation plane with respect to frame $\boldsymbol{H}$, the Euler angles θ_x, θ_y would keep constant here. The sensor noise is taken as Gauss white noise here, and the initial relative states error is chosen as

$$\boldsymbol{e} = \left[-0.5, 0.2, 0.6\right]^{\mathrm{T}} \text{ m}, \ \dot{\boldsymbol{e}} = \left[0.06, 0.01, -0.04\right]^{\mathrm{T}} \text{ m s}^{-1}.$$

Time histories of the feed-forward electromagnetic control forces and the corresponding magnetic dipoles on *Sat*B are presented in Figure 6. It is obvious that both profiles for feed-forward electromagnetic forces and magnetic dipoles are smooth and periodic.

The design parameters of the modified ESO are selected as

$$\alpha_1 = 0.5, \ \alpha_2 = 0.25, \ \alpha_3 = 0.125, \delta_1 = \delta_2 = \delta_3 = 0.05$$
$$\beta_0 = 150, \ \beta_1 = 300, \ \beta_2 = 600, \ \beta_3 = 1600, \ \tau = 0.02.$$

The nonlinear states error feedback controller is specified to be

$$\lambda = 0.03, \ \varepsilon = 2\times10^{-4}, \ \kappa = 6\times10^{-3}, \rho = 0.01.$$

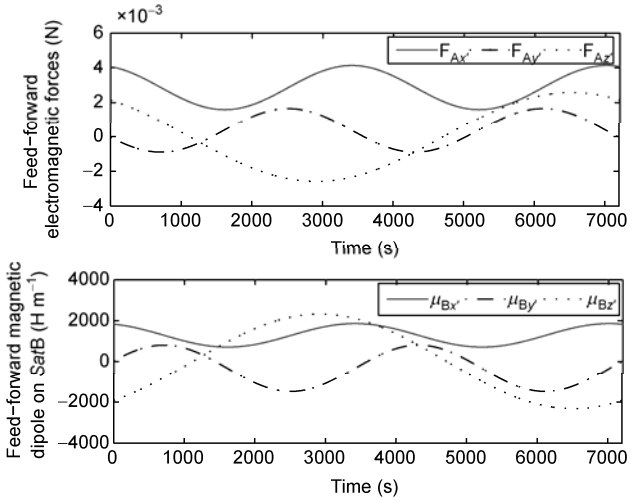

Figure 6 Feed-forward control component.

The desired transient profile and its tracking error are illustrated in Figures 7–9 respectively. It can be seen that the real configuration deviation tracks the desired profile well

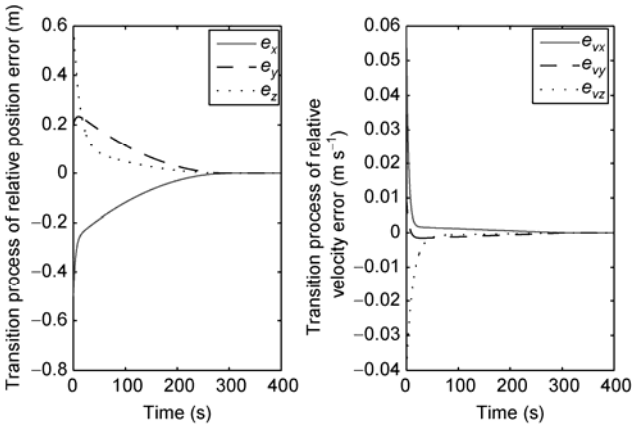

Figure 7 Desired transient profile.

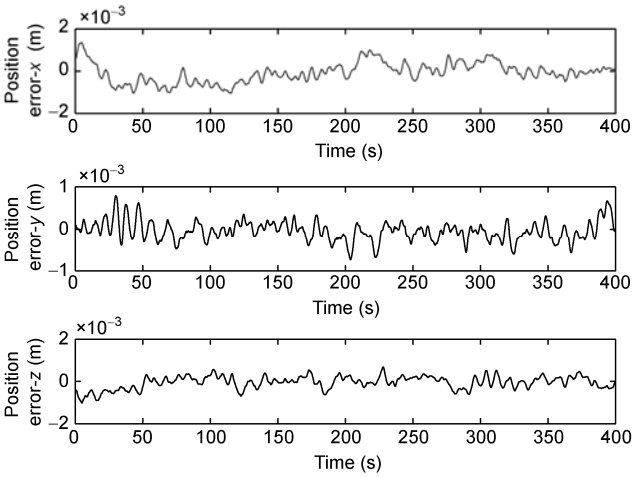

Figure 8 Tracking error for the desired transient profile of relative position error.

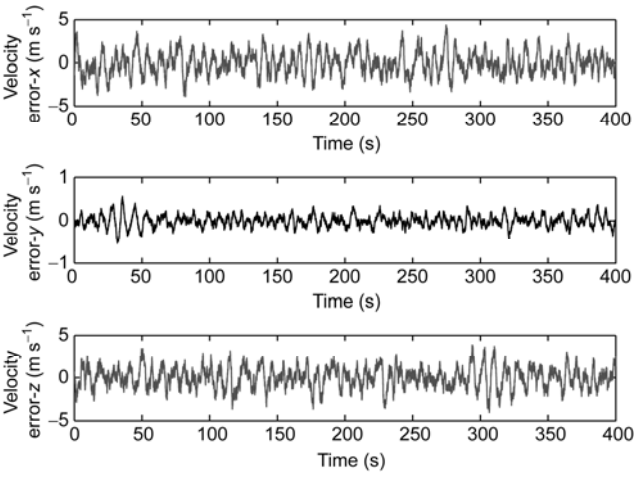

Figure 9 Tracking error for the desired transient profile of relative velocity error.

and converges to zero in the end, validating the feasibility of our feedback control component. The error feedback control inputs in both forms of electromagnetic force and magnetic dipole strength are presented in Figures 10–12. The magnitude of the control forces is small enough, applicable to electromagnetic coils on the satellite; and the chatter is produced by compensating for the sensor noise.

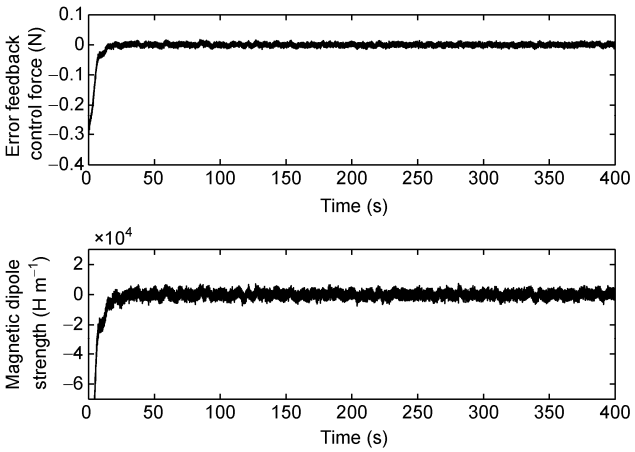

Figure 10 Feedback control component in x' axis.

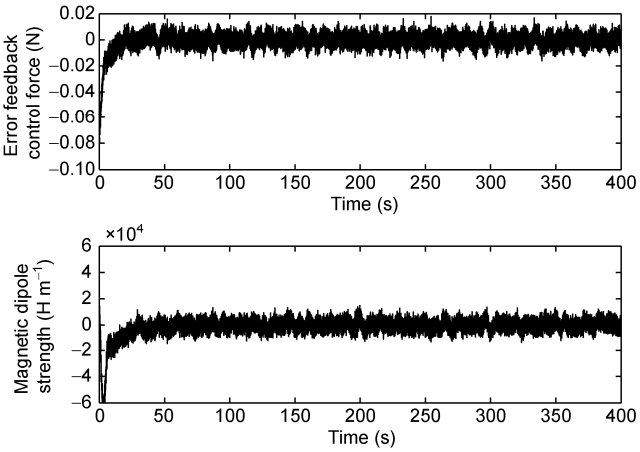

Figure 11 Feedback control component in y' axis.

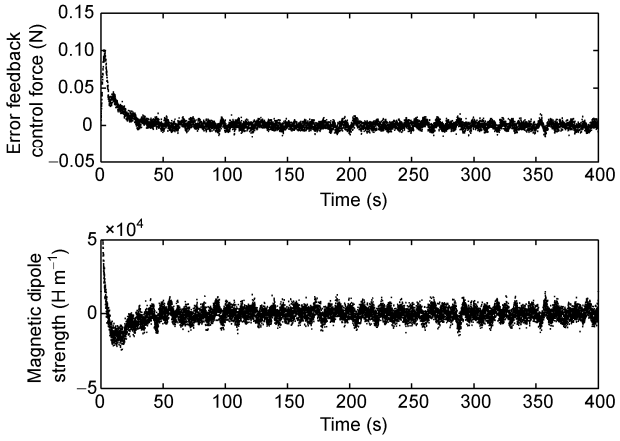

Figure 12 Feedback control component in z' axis.

5 Conclusions

Concentrating on the formation keeping control through inter-satellite electromagnetic force, this paper analyzes the dynamic characteristic and special control challenges brought by the electromagnetic force, and studies the nonlinear control issues with a combined control strategy. Some useful conclusions are drawn as follows. Firstly, the internal force nature of electromagnetic force yields coupled motion between electromagnetic satellites, and the electromagnetic force has high nonlinearity with respect to the relative separation and orientation of magnetic dipoles. The uncertainties of the far-field electromagnetic force model and geomagnetic influence should be taken into account in designing the formation keeping controller. Secondly, the combined formation keeping controller including feed-forward and feedback control components could be designed utilizing ADRC methodology, exhibiting good robust capability to model uncertainties and external disturbances, as well as sensor noise. Thirdly, this paper has conducted a primary research on the control problem of relatively translational motion via inter-satellite electromagnetic force. Such issues as synchronous control of electromagnetic satellites considering the coupling in relatively translational and attitude dynamics, angular momentum management strategy for EMFF may be potential fields to explore in the future.

This work was supported by the National Natural Science Foundation of China (Grant No. 11172322) and the authors would like to thank Ms. Peng WangQiong for her helpful suggestions in this English manuscript.

1 Kwon D W. Propellantless formation flight applications using electromagnetic satellite formations. Acta Astronaut, 2010, 67: 1189–1201
2 Schweighart S A, Sedwick R J. Explicit dipole trajectory solution for electromagnetically controlled spacecraft clusters. J Guid Control Dynam, 2010, 33: 1225–1235
3 Elias L M. Dynamics of multi-body space interferometers including reaction wheel gyroscopic stiffening effects: Structurally connected and electromagnetic formation flying architectures. Doctoral Dissertation. Massachusetts: Massachusetts Institute of Technology, 2004
4 Ahsun U. Dynamics and control of electromagnetic satellite formations. Doctoral Dissertation. Massachusetts: Massachusetts Institute of Technology, 2007
5 Ahsun U, Miller D W, Ramirez J L. Control of electromagnetic satellite formations in near-Earth orbits. J Guid Control Dynam, 2010, 33: 1883–1891
6 Kwon D W, Sedwick R J, Lee S-i, et al. Electromagnetic formation flight testbed using superconducting coils. J Spacecr Rock, 2011, 48: 124–134
7 Neave M. Dynamic and thermal control of an electromagnetic formation flight testbed. Dissertation for Master Degree. Massachusetts: Massachusetts Institute of Technology, 2005
8 Kaneda R, Yazaki F, Sakai S-i, et al. The relative position control in formation flying satellites using super-conducting magnets. In: Pro-

ceedings of the 2nd International Symposium on Formation Flying Missions & Technologies. Washington D.C., 2004
9 Wawrzaszek R, Banaszkiewicz M. Control and reconfiguration of satellite formations by electromagnetic forces. J Telecom Inf Technol, 2007, 1: 54–58
10 Zeng G Q, Hu M. Finite-time control for electromagnetic satellite formations. Acta Astronaut, 2012, 74: 120–130
11 Feng C T, Wang H N, Liu H Y, et al. Nonlinear control for electromagnetic formation flight of multi-satellites (in Chinese). Transd Microsyst Technol, 2009, 28: 54–59
12 Su J M, Dong Y F. Sliding mode variable structure control for electromagnetic satellite formation station-tracking (in Chinese). J Aeronaut, 2011, 32: 1093–1099
13 Mackison D L. Identification and adaptive control of a satellite flight control system. In: Proceedings of the Astrodynamics Specialist Conference and Exhibit. Monterey: AIAA/AAS, 2002. 1–8
14 Massey T, Shtessel Y. Satellite formation control using traditional and high order sliding modes. In: Proceedings of the Guidance, Navigation, and Control Conference and Exhibit. Rhode Island: AIAA, 2004. 1–20
15 Liu H, Li J F, Hexi B Y. Sliding mode control for low-thrust Earth-orbiting spacecraft formation maneuvering. Aerosp Sci Technol, 2006, 10: 636–643
16 Li Z K, Duan Z S. Distributed adaptive attitude synchronization of multiple spacecraft. Sci China Tech Sci, 2011, 54: 1992–1998
17 Schlanbusch R, Kristiansen R, Nicklasson P J. Spacecraft formation reconfiguration with collision avoidance. Automatica, 2011, 47: 1443–1449
18 Han J. From PID to active disturbance rejection control. IEEE T Indust Elec, 2009, 56: 900–906
19 Xiong H, Yi J Q, Fan G L, et al. Anti-crosswind autolanding of UAVs based on active disturbance rejection control. In: Proceedings of the Guidance, Navigation, and Control Conference. Toronto: AIAA, 2010. 1–14
20 Li S, Yang X, Yang D. Active disturbance rejection control for high pointing accuracy and rotation speed. Automatica, 2009, 45: 1854–1860
21 Yao Y, Wang Y H. Acceleration estimation of maneuvering targets based on extended state observer (in Chinese). Syst Eng Elec, 2009, 31: 2682–2685
22 Ahsun U. Using electromagnetic formation flying for remote sensing applications. In: Proceedings of the 2nd International Conference on Advances in Space Technologies. Islamabad: IAF, 2008. 118–123